Solid State Ionics 181 (2010) 1183–1188

Contents lists available at ScienceDirect

Solid State Ionics

journal homepage: www.elsevier.com/locate/ssi

Hybrid inorganic–organic proton exchange membranes containing 1*H*-1,2,3-triazole moieties

Shilpi Sanghi [a], Mark Tuominen [b], E. Bryan Coughlin [a,*]

[a] Department of Polymer Science and Engineering, University of Massachusetts, Amherst, MA 01003, USA
[b] Department of Physics, University of Massachusetts, Amherst, MA 01003, USA

ARTICLE INFO

Article history:
Received 9 February 2010
Received in revised form 22 June 2010
Accepted 24 June 2010

Keywords:
1,2,3-Triazole
Sol–gel
Inorganic–organic hybrids

ABSTRACT

Hybrid inorganic–organic polymer electrolyte membranes (PEM) were synthesized from a combination of 1*H*-1,2,3-triazole grafted alkoxy silanes, tetraethoxy silane (TEOS), polyethylene glycol (PEG) and trifluoroacetic acid (TFA) or phosphoric acid. The resulting hybrid inorganic–organic proton exchange membranes were self-supporting and thermally stable up to 180 °C. Evaluation of proton conductivity as a function of temperature indicates that by using sol–gel chemistry, it is possible to achieve mechanically robust membranes having proton conductivity comparable to uncrosslinked, liquid-like 1*H*-1,2,3-triazole functionalized polysiloxane homopolymer. Mechanical properties of these hybrid inorganic–organic membranes were investigated using nanoindentation.

1. Introduction

Great strides have been made in the past few years in the progress of proton exchange membranes for fuel cells. The development of a proton exchange membrane with high mechanical strength, thermal, chemical and electrochemical stability and proton conductivity with little dependence on water is an important challenge in the large scale commercialization of proton exchange membrane fuel cells (PEMFCs) [1]. The present state-of-the-art membrane technology is based on perfluorosulfonic acid (PFSA) membranes whose operating temperature is limited to 80 °C as water is the medium for proton transport [2–4]. Operation of a fuel cell at temperatures above 120 °C has the advantages of reduced platinum loading, improved tolerance to CO, enhanced electrochemical reactions, simplified water and thermal management design. This reduces the overall cost of fuel cells [5].

Intensive research efforts have been made to achieve anhydrous proton conduction by replacing water with heterocycles, e.g., imidazole, benzimidazole [6–9]. In these amphoteric nitrogen containing heterocycles, proton transport takes place through a hydrogen bonded network of heterocycles by a hydrogen bond breaking and formation process [10,11]. Previously, the proton conducting properties of poly(acrylates), poly(siloxanes) and poly(phosphazenes) with pendant 1*H*-1,2,3-triazole as a protogenic group have been studied in our group [12–15]. The amorphous nature of these low T_g polymers allows for high local mobility of triazoles, thereby giving proton conductivity in the range of 0.01–1 μS/cm at 180 °C; however, they do not form self-supporting membranes. For efficient fuel cell operation, membranes must be mechanically robust. Developing a membrane with good mechanical properties along with high conductivity is a challenge.

The proton exchange membranes can be mechanically reinforced by crosslinking or nano-confinement in a porous medium [16–19]. Li et al. reported mechanically robust hybrid inorganic–organic membranes containing condensed organosilicon precursors with grafted imidazole and benzimidazole. These membranes were shown to have conductivity of the order of 10^{-3} S/cm at 120 °C after doping with H_3PO_4 [20]. Similarly, membranes composed of benzimidazole covalently bonded to an inorganic SiO_2 network by a flexible spacer were investigated by Herz et al. [21]. Furthermore, Li and coworkers reported that the grafting of 1*H*-1,2,4-triazole onto a hybrid inorganic–organic polymer network enhances the proton conductivity of the hybrid membranes doped with H_3PO_4 [22].

In the present work, we have focused on structural reinforcement of 1*H*-1,2,3-triazole functionalized poly(siloxane); a low T_g polymer, by crosslinking using sol–gel chemistry [23]. The macroscopic and microscopic proton conduction behaviors of 1*H*-1,2,3-triazole functionalized poly(siloxane) (Tz5Si) were reported recently [24]. In this work, we have studied the effect of crosslinking on proton conductivity and mechanical properties of triazole functionalized poly(siloxane) which has the same spacer length between triazole and polymer backbone as that of the previously reported Tz5Si.

2. Experimental

2.1. Materials

Allyl bromide, propargyl alcohol, sodium hydride, chloromethyl pivalate, sodium azide, tetraethoxy silane (TEOS), triethoxy silane,

* Corresponding author. Tel.: +1 4135771616; fax: +1 4135450082.
E-mail address: Coughlin@mail.pse.umass.edu (E.B. Coughlin).

0167-2738/$ – see front matter © 2010 Elsevier B.V. All rights reserved.
doi:10.1016/j.ssi.2010.06.051

copper(II) sulfate ($CuSO_4 \cdot 5H_2O$), sodium ascorbate, t-butanol (t-BuOH), Karstedt's catalyst, trifluoroacetic acid (TFA), phosphoric acid and hydroxyl terminated polyethylene glycol (PEG) (M_n ~300 g/mol) were purchased from Sigma-Aldrich or VWR and used as received. Azidomethyl pivalate was prepared as reported in the literature [25].

2.2. Characterization

^{1}H NMR (300 MHz) and ^{13}C NMR (75 MHz) spectra were obtained on a Bruker DPX-300 NMR spectrometer. Fourier-transform infrared (FT-IR) spectra were obtained using a Perkin Elmer Spectrometer. Thermogravimetric analysis (TGA) was performed using a TA instrument TGA 2950 thermogravimetric analyzer at a heating rate of 10 °C/min under nitrogen flow of 20 mL/min. Glass transition temperatures were obtained using TA instrument DSC 2910 differential scanning calorimeter (DSC) by heating the samples at a rate of 10 °C/min under nitrogen flow (50 mL/min). Electrochemical impedance data was obtained using a Solatron 1287 potentiostat/1252A frequency response analyzer. Measurements were done by pressing the polymer samples between two gold coated blocking electrodes followed by an application of 100 mV excitation voltage with a logarithmic frequency sweep from 3×10^5 to 1×10^{-1} Hz under vacuum to ensure an anhydrous environment. Z″ vs. Z′ plot was used to determine the resistance values at the minimum imaginary response [26]. A Hysitron Triboindenter was used for nanoindentation studies.

2.3. Synthesis

3-Allyloxyprop-1-yne **(1)** and 4-(allyloxymethyl)-[1,2,3]triazol-1-ylmethyl pivalate **(3)** were synthesized as previously reported [24]. 2,2-Dimethyl-propionic acid-4-(3-triethoxysilylpropyloxymethyl)-[1,2,3]triazol-1-ylmethyl ester **(4)** (Tz5TrS) was synthesized by Pt^0 catalyzed hydrosilylation reaction. In a dry box, 159 mg (0.63 mmol) of **(2)**, 154 mg (0.94 mmol) of triethoxysilane and 0.38 mL of toluene (4 M) were combined in a small reaction vial equipped with a magnetic stirrer. The mixture was stirred for 5 min followed by an addition of 5 drops of Karstedt's catalyst. The vial was then removed from the dry box and stirred at 70 °C for 2 days. The solvent was removed under vacuum and the resulting product was an oily yellow liquid. It was used without further purification as exposure to moisture leads to hydrolysis of alkoxysilyl groups. ^{1}H NMR ($CDCl_3$): δ 1.2 (s, 9H), 1.28–1.42 (m, 9H), 1.85 (m, 2H), 3.6 (t, 2H), 3.9–4.05 (m, 6H), 4.73 (s, 2H), 6.2 (s, 2H), 7.85 (s, 1H). ^{13}C NMR ($CDCl_3$): δ 6.53, 18.35, 26.85, 38.82, 64.14, 69.16, 73.18, 123.84, 146.16, 177.80.

2.4. Preparation of membranes

The first step involved removal of the pivaloxymethyl (POM) protecting group from the precursor by using sodium methoxide. Precursor Tz5TrS-POM (0.3 g, 0.7 mmol), ethylene diamine (75 μL, 1.12 mmol) and 0.1 M NaOH/MeOH (10.5 mL, 1.05 mmol) were combined in a vial and allowed to stir for 2 h. The reaction mixture was then concentrated to half of its original volume by rotary evaporation. The pH of the solution was adjusted to 4 using a 1 M solution of HCl followed by addition of TEOS and PEG. The mixture was allowed to stir at room temperature for at least 12 h. Then TFA or H_3PO_4 was added and the solution was allowed to stir for 2 h to form uniform sols. Films were then cast and dried in a stepwise manner; 24 h at room temperature and atmospheric pressure followed by drying under vacuum at room temperature for 24 h, then 55 °C–60 °C for 2 days, 80 °C for 3 h and then finally at 100 °C for 2 h to evaporate organic solvents and water. These membranes were stored under vacuum at 30 °C as they are hygroscopic in nature. The samples are labeled by their mole composition as xPEG-yTEOS-zTz5TrS-aTFA-bP where x,y,z,a,b refer to moles of PEG, TEOS, precursor Tz5TrS, TFA and H_3PO_4 respectively.

3. Results and discussion

3.1. Synthesis

Azide-alkyne Hüsgen 1,3-dipolar cycloaddition reaction, “click” chemistry, was used to synthesize **(3)** as per the literature procedure [24]. The Pt^0 catalyzed hydrosilylation reaction between Si—H bond of triethoxy silane and vinyl group of **(3)** gave the sol–gel monomer **(4)** (Scheme 1). The triazole terminated sol–gel monomer **(4)** was deprotected and then crosslinked with tetraethoxy silane (TEOS) and poly(ethylene glycol) (PEG) by hydrolysis and condensation in the presence of acidified water (Scheme 2), PEG being a flexible spacer, reduces shrinkage during drying and brittleness of the membrane [19]. In order to confirm that PEG is covalently bonded in the crosslinked network, a 1PEG-1TEOS-1Tz5TrS film was submerged in D_2O at room temperature for 2 d. ^{1}H NMR analysis of that D_2O showed no presence of PEG indicating that PEG is covalently bonded and not just trapped within the network as a dopant. All the membranes studied have residual ethylene diamine and NaCl from the deprotection step to remove the pivalate group. These byproducts were not removed by washing of membranes with water as that will lead to leaching of doped acid as well, making it difficult to quantify the amount of acid present in the material. At the same time, acid doping cannot be done after crosslinking and washing steps, due to the insolubility of the crosslinked membranes.

3.2. FT-IR study

The removal of the POM-protecting group from triazole tethered to siloxane was confirmed by FT-IR spectrum of condensed Tz5TrS membrane. The C O group absorption at 1740 cm^{-1} in protected Tz5TrS disappeared after deprotection indicating complete removal of POM group. The deprotection was also confirmed by the presence of

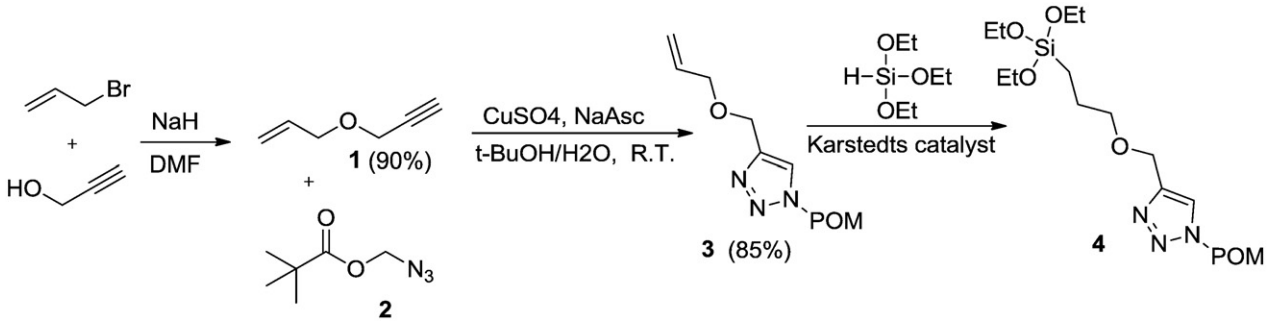

Scheme 1. Synthetic route to 2,2-dimethyl-propionic acid-4-(3-triethoxysilylpropyloxymethyl)-[1,2,3]triazol-1-ylmethyl ester (Tz5TrS). [Pivaloxymethyl group is abbreviated as POM].

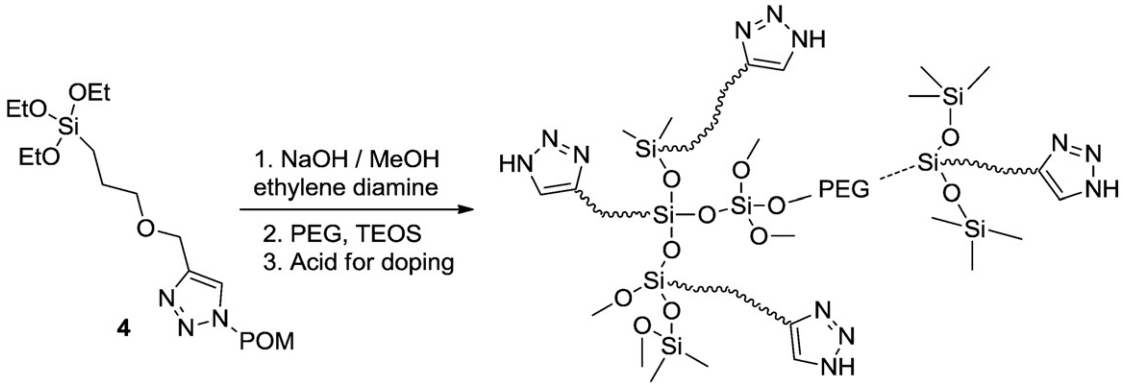

Scheme 2. Preparation of hybrid inorganic–organic copolymer.

N—H group absorption at 3424 cm^{-1}. Fig. 1 shows the IR spectra of condensed Tz5TrS before and after deprotection.

3.3. Thermal properties

Thermogravimetric analysis has shown that all the materials are stable up to 180 °C under nitrogen. The small weight loss below the decomposition temperature is due to the loss of water and solvents which tend to remain in the membrane. The onset of decomposition, temperature corresponding to 5% weight loss and glass transition temperatures of all the samples are summarized in Table 1. All the polymers show a single T_g. The T_g of condensed Tz5TrS is higher than that of other materials due to the restricted segmental relaxation in the crosslinked network. As expected, the T_g of PEG containing hybrid membranes is lower. Also, addition of acid leads to lowering of T_g due to a plasticization effect.

3.4. Appearance of hybrid inorganic–organic membranes

Free-standing membranes with thicknesses in between 100 μm and 150 μm were obtained. Membranes without PEG were stiff and brittle. Addition of PEG imparts flexibility to these membranes, as highly flexible ethylene oxide chains connect the three dimensional Si—O—Si network. Membranes shown in Fig. 2 are self-supporting.

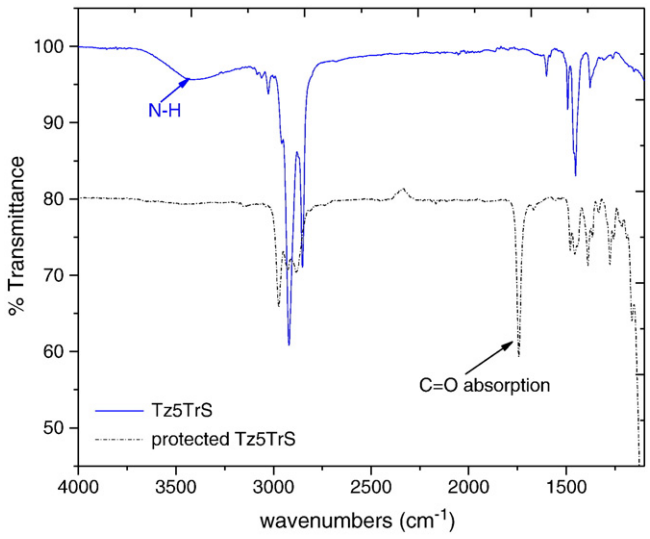

Fig. 1. FT-IR spectra of condensed Tz5TrS.

3.5. Proton conductivity

3.5.1. Proton conductivity of 1H-1, 2, 3-triazole grafted condensed organosilicon precursor

The temperature dependent proton conductivity of condensed sol–gel monomer Tz5TrS, before and after doping with TFA or H_3PO_4 was measured and compared with the previously reported linear homopolymer Tz5Si which has the same tether length as Tz5TrS, Fig. 3 [24]. The conductivity of condensed Tz5TrS is three orders of magnitude lower than that of homopolymer Tz5Si. This is because the dominant conduction process in triazole functionalized membranes is structural diffusion, which involves intermolecular proton transfer and reorganization by a hydrogen bond breaking and forming process, and as a result proton conductivity depends on the local mobility of the matrix [27–29]. In condensed Tz5TrS, the tight Si—O—Si crosslinked network reduces the chain mobility as reflected by the higher glass transition temperature of condensed Tz5TrS ($T_g = 47$ °C) compared to that of homopolymer Tz5Si ($T_g = 5$ °C). The proton conductivity of the condensed Tz5TrS after doping with TFA or H_3PO_4 is comparable to the homopolymer Tz5Si, since conductivity depends upon both the mobility and the charge carrier density. Addition of acid introduces extrinsic charge carriers leading to an increase in conductivity. An increase in conductivity of up to 2 orders of magnitude after doping with TFA has been reported previously [12,13]. At the highest temperature measured, the improvement in conductivity with H_3PO_4 doping is even greater that that observed for TFA doping. However, membranes comprising condensed Tz5TrS, both doped and undoped, are rigid and fragile, and lack the flexibility needed to be used as proton exchange membrane in fuel cells.

3.5.2. Proton conductivity of hybrid inorganic–organic membranes

The proton conductivity of the hybrid inorganic–organic membranes, 1PEG-1TEOS-1Tz5TrS-1TFA and 1PEG-1TEOS-1Tz5TrS-2.5P,

Table 1
Thermal properties of the materials studied.

Material	T_g (°C)[a]	Triazole mass fraction (wt.%)[b]	T_{d5} (°C)[c]
Condensed Tz5TrS	47	33	204
1TzTrS-TFA	29	21	205
1TzTrS-2.5P	23	15	189
1PEG-1TEOS-1Tz5TrS-2.5P	−12	8	182
1PEG-1TEOS-1Tz5TrS-1TFA	−19	10	206
Tz5Si[d]	5	34	

[a] Obtained from DSC on the second heating cycle.
[b] Mass fraction of triazole in the heterocycle matrix is calculated after accounting for the weight of the doped acid.
[c] 5% weight loss as determined by TGA with a heating rate of 10 °C/min from room temperature to 500 °C under N_2.
[d] Thermal properties of Tz5Si from the literature [24].

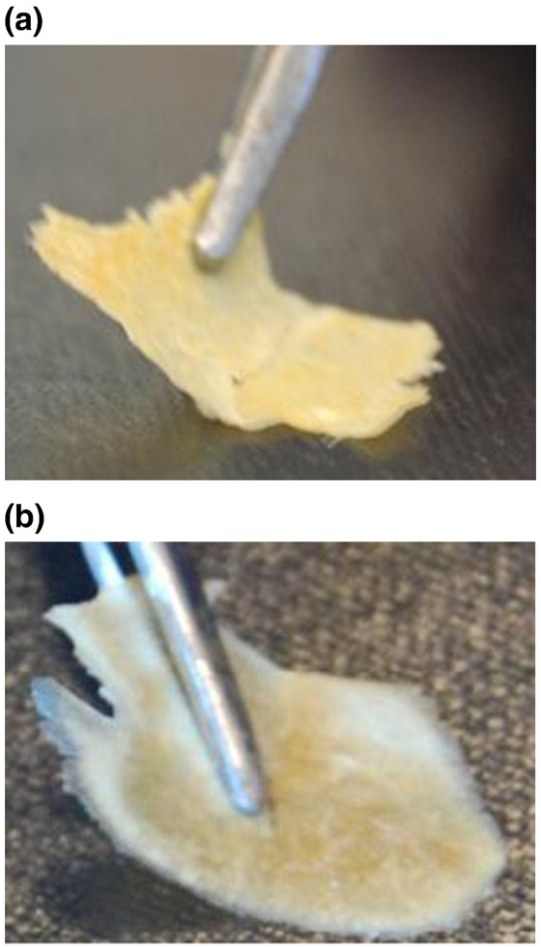

Fig. 2. Appearance of membranes. a) 1PEG-1TEOS-1Tz5TrS-1TFA. b) 1PEG-1TEOS-1Tz5TrS-2.5P.

increases with increasing temperature, reaching 1.6 mS/cm at 180 °C for 1PEG-1TEOS-1Tz5TrS-2.5P, Fig. 4. These conductivities are slightly higher than that of the homopolymer Tz5Si [24]. Although the high temperature proton conductivity of the two membranes doped with TFA or H_3PO_4 at 180 °C is similar, the shape of the Log (σ) vs. 1000/T curves is different suggesting a difference in proton transport mechanism. This could be explained by the fact that H_3PO_4 molecules interact quantitatively with the protogenic group and so an excess of H_3PO_4 to triazole group is necessary to give sufficient proton conductivity [30]. When H_3PO_4 is used as a dopant, another conduction mechanism is also possible; proton transport taking place along a $H_2PO_4^-/HPO_4^{2-}$ anionic chain by consecutive proton transfer between phosphate species and anion reorientation steps [20,31,32]. In TFA doped materials, maximum ion conductivity is attributed to the proton exchange between protonated and non-protonated heterocycle sites [32].

3.6. Mechanical properties

The mechanical properties of the membranes were studied using nanoindentation [33]. Condensed Tz5TrS, 1Tz5TrS-1TFA and 1Tz5TrS-2.5P were too fragile for mechanical testing. Only the mechanical properties of PEG containing membranes were studied, and were compared to that of hydrated Nafion-112.

A peak load of 20 μN was applied at a rate of 4 μN/s and then sample was held under maximum load for 5 s, followed by unloading at the same rate of 4 μN/s. During the indentation process, the penetration depth (h) was measured and the area of the indent (A) was determined using the known geometry of the indentation tip. The indenter was a diamond Berkovich (or triagonal pyramid) geometry with a geometric constant (ε) of 0.75, center to face angle of 65.35° and tip radius ~ 150 nm as quoted by the manufacturer. The modulus of the samples was obtained from the unloading portion of the curve by plotting load vs. displacement and then using Oliver and Pharr analysis [33]. The load vs. displacement curves of the samples studied are shown in Fig. 5. The slope of the unloading curve at the maximum loading point (h_{max}) gave the contact stiffness of the material, Eq. (1). Knowing the projected area of the tip-sample contact A_c, at the peak load P_{max}, and the stiffness S at the onset of loading, the reduced modulus, E_r was calculated by Eq. (2). Since an elastic displacement occurs both in the specimen and the indenter; reduced modulus accounts for deformation of both the indenter and the sample and is related to the Young's modulus of the specimen E_s, by Eq. (3); where E_s and ν_s are Young's modulus and Poisson's ratio for the specimen and E_i and ν_i are the same parameters for the indenter (diamond in this case) [33,34].

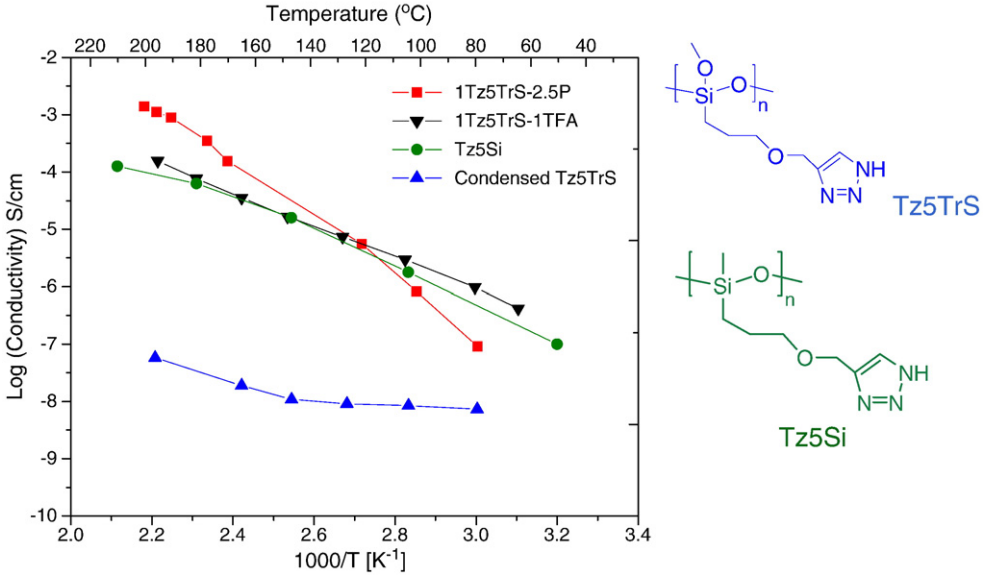

Fig. 3. Proton conductivity vs. temperature for condensed Tz5TrS, Tz5TrS-1TFA, and Tz5TrS-2.5P along with Tz5Si for comparison [24].

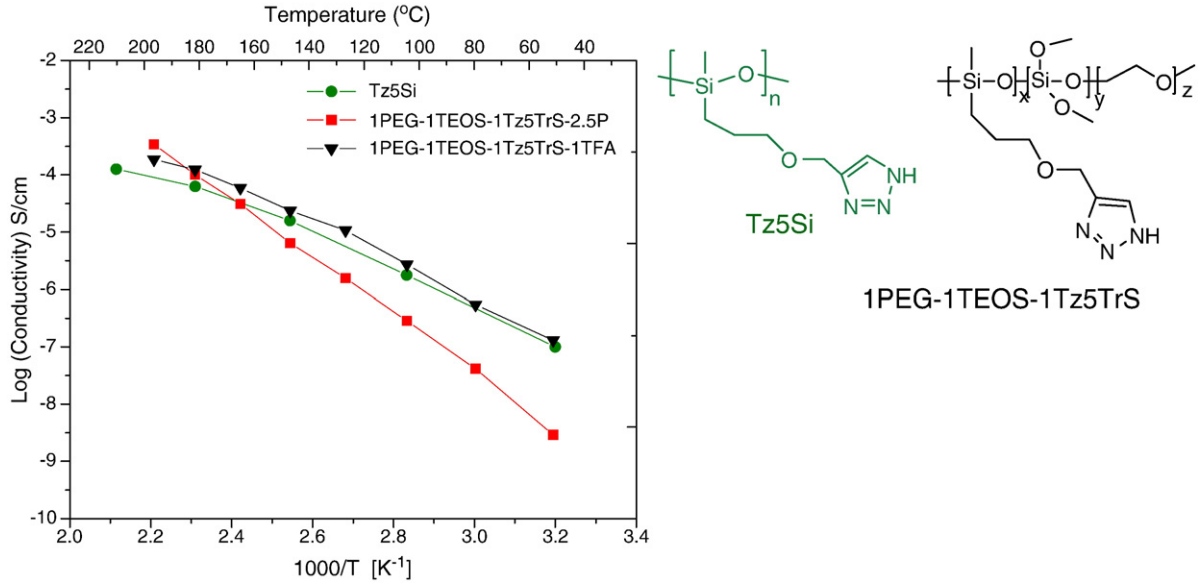

Fig. 4. Proton conductivity of 1PEG-1TEOS-1Tz5TrS-1TFA and 1PEG-1TEOS-1Tz5TrS-2.5P along with Tz5Si for comparison [24].

Contact stiffness

$$S = \frac{dP}{dh}\,|h_{\max} \tag{1}$$

Reduced modulus

$$E_r = \frac{\sqrt{\pi}}{2}\frac{1}{\sqrt{A_c}}S \tag{2}$$

Sample's elastic (Young's) modulus, E_s

$$E_{sample} = \left(1-\nu_s^2\right) / \left(\frac{1}{E_r} - \frac{1-\nu_i^2}{E_i}\right) \tag{3}$$

($E_i = 1141$ GPa, $\nu_i = 0.07$ for diamond).

The reduced moduli of 1PEG-1TEOS-1Tz5TrS-1TFA, 1PEG-1TEOS-1Tz5TrS-2.5P and Nafion were found to be 139 MPa, 315 MPa and 765 MPa respectively. The modulus of TFA doped membrane is approximately one fifth that of Nafion, while modulus of H_3PO_4 doped membrane is approximately half that of Nafion. The membrane doped with H_3PO_4 was stronger than that doped with TFA.

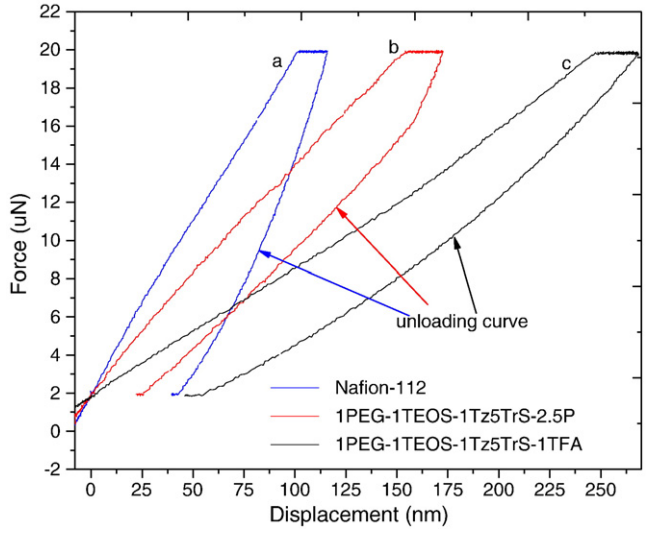

Fig. 5. Load vs. displacement curve. a) Nafion-112. b) 1PEG-1TEOS-1Tz5TrS-2.5P. c) 1PEG-1TEOS-1Tz5TrS-1TFA.

For polymers, the Oliver and Pharr analysis overestimates the modulus compared to the macroscopic Young's elastic modulus, as polymers creep, being viscoelastic in nature, while the Oliver and Pharr model analyzes the load–displacement curve with elastic contact mechanics models [35,36]. The modulus obtained by this analysis may be greater than the actual values, the relative comparison with Nafion would be similar. From the reduced modulus of Nafion (765 MPa), its Young's modulus was calculated as 643 MPa using Eq. (3) ($\upsilon = 0.4$ for Nafion) [37]. The Young's modulus of Nafion obtained by DMA (dynamic mechanical analyzer) for similar hydration levels was reported as 437 MPa [38].

4. Conclusion

The anhydrous proton conducting, low T_g triazole functionalized poly(siloxane) was mechanically reinforced by crosslinking using sol–gel technique. The resulting hybrid inorganic–organic membranes are self-supporting and thermally stable up to 180 °C. The incorporation of PEG imparts flexibility to the crosslinked membrane. Crosslinking leads to a decrease in conductivity due to the restricted local mobility of the triazole group. However, addition of acid helps restore the conductivity of crosslinked membranes up to $10^{-2.5}$ S/cm at 180 °C which is slightly greater than that of the uncrosslinked, low T_g homopolymer and the same as that of acid doped homopolymer. Compared to the organic polymer containing acid, the hybrid inorganic–organic copolymer membranes containing acid can achieve high proton conductivity along with good mechanical properties.

Acknowledgements

Funding was provided by the NSF Center for Chemical Innovation at UMass Amherst, Grant #CHE-0739227. Analytical facilities were made available through the NSF-supported Materials and Research Science and Engineering Center on Polymers at UMass Amherst. The authors would like to thank Chelsea Davis for helpful suggestions and insightful comments on mechanical testing.

References

[1] L. Carrette, K.A. Friedrich, U. Stimming, Fuel Cells 1 (1) (2001) 5.
[2] M. Hickner, H. Ghassemi, Y. Kim, B. Einsla, J. McGrath, Chem. Rev. 104 (2004) 4587.
[3] S.J. Hamrock, M.A. Yandrasits, J. Macromol. Sci., Part C: Polym. Rev. 46 (3) (2006) 219.
[4] B. Smitha, S. Sridhar, A.A. Khan, J. Membr. Sci. 259 (1–2) (2005) 10.
[5] Q. Li, R. He, J.O. Jensen, N.J. Bjerrum, Chem. Mater. 15 (26) (2003) 4896.
[6] M.F.H. Schuster, W.H. Meyer, M. Schuster, K.D. Kreuer, Chem. Mater. 16 (2) (2004) 329.
[7] J.C. Persson, P. Jannasch, Macromolecules 38 (8) (2005) 3283.
[8] M. Schuster, W.H. Meyer, G. Wegner, H.G. Herz, M. Ise, M. Schuster, K.D. Kreuer, J. Maier, Solid State Ionics 145 (1–4) (2001) 85.
[9] R.C. Woudenberg, O. Yavuzcetin, M.T. Tuominen, E.B. Coughlin, Solid State Ionics 178 (15–18) (2007) 1135.
[10] W. Münch, K.D. Kreuer, W. Silvestri, J. Maier, G. Seifert, Solid State Ionics 145 (1–4) (2001) 437.
[11] K.-D. Kreuer, Chem. Mater. 8 (3) (1996) 610.
[12] S. Granados-Focil, R.C. Woudenberg, O. Yavuzcetin, M.T. Tuominen, E.B. Coughlin, Macromolecules 40 (24) (2007) 8708.
[13] S. Martwiset, R.C. Woudenberg, S. Granados-Focil, O. Yavuzcetin, M.T. Tuominen, E.B. Coughlin, Solid State Ionics 178 (23–24) (2007) 1398.
[14] S. Martwiset, O. Yavuzcetin, M. Thorn, C. Versek, M. Tuominen, E.B. Coughlin, J. Polym. Sci.,Part A: Polym. Chem. 47 (1) (2009) 188.
[15] M. Higami, R.C. Woudenberg, S. Granados-Focil, O. Yavuzcetin, M.T. Tuominen, E.B. Coughlin, PMSE Preprints, 2007, p. 551.
[16] H. Chen, G.R. Palmese, Y.A. Elabd, Chem. Mater. 18 (20) (2006) 4875.
[17] T. Tezuka, K. Tadanaga, A. Hayashi, M. Tatsumisago, J. Am. Chem. Soc. 128 (51) (2006) 16470.
[18] T. Tezuka, K. Tadanaga, A. Hayashi, M. Tatsumisago, Solid State Ionics 179 (21–26) (2008) 1151.
[19] S. Li, Z. Zhou, H. Abernathy, M. Liu, W. Li, J. Ukai, K. Hase, M. Nakanishi, J. Mater. Chem. 16 (2006) 858.
[20] S. Li, Z. Zhou, M. Liu, W. Li, J. Ukai, K. Hase, M. Nakanishi, Electrochim. Acta 51 (7) (2006) 1351.
[21] H.G. Herz, K.D. Kreuer, J. Maier, G. Scharfenberger, M.F.H. Schuster, W.H. Meyer, Electrochim. Acta 48 (14–16) (2003) 2165.
[22] S. Li, Z. Zhou, Y. Zhang, M. Liu, W. Li, Chem. Mater. 17 (24) (2005) 5884.
[23] J.D. Wright, N.A.J.M. Sommerdijk, Sol–Gel Materials: Chemistry and Applications, CRC Press, London, 2001, p. 15.
[24] Ü. Akbey, S. Granados-Focil, E.B. Coughlin, R. Graf, H.W. Spiess, J. Phys. Chem. B 113 (27) (2009) 9151.
[25] J.C. Loren, A. Krasinski, V.V. Fokin, K.B. Sharpless, Synlett 18 (2005) 2847.
[26] J.R. MacCallum, C.A. Vincent, Polymer Electrolyte Reviews, 1, Elsevier Applied Science, New York, 1987, p. 237.
[27] R. Subbaraman, H. Ghassemi, T.A.J. Zawodzinski, J. Am. Chem. Soc. 129 (8) (2007) 2238.
[28] Z. Zhou, R. Liu, J. Wang, S. Li, M. Liu, J.-L. Bredas, J. Phys. Chem. A 110 (7) (2006) 2322.
[29] G. Scharfenberger, W.H. Meyer, G. Wegner, M. Schuster, K.D. Kreuer, J. Maier, Fuel Cells 6 (3–4) (2006) 237.
[30] M. Rikukawa, K. Sanui, Prog. Polym. Sci. 25 (10) (2000) 1463.
[31] K.D. Kreuer, J. Membr. Sci. 185 (1) (2001) 29.
[32] P. Colomban, Proton Conductors: Solids, Membranes and Gels—Materials and Devices, 2, Cambridge University Press, Cambridge, 1992, p. 311.
[33] W.C. Oliver, G.M. Pharr, J. Mater. Res. 7 (6) (1992) 1564.
[34] M.R. VanLandingham, J.S. Villarrubia, W.F. Guthrie, G.F. Meyers, Macromol. Symp. 167 (2001) 15.
[35] T. Davide, P. Stefano, L. Joachim, A. Alexander, Macromolecules 40 (4) (2007) 1259.
[36] J.M. Kranenburg, C.A. Tweedie, K.J.v. Vliet, U.S. Schubert, Adv. Mater. 21 (35) (2009) 3551.
[37] R. Solasi, Y. Zou, X. Huang, K. Reifsnider, D. Condit, J. Power Sources 167 (2) (2007) 366.
[38] S. Kundu, L.C. Simon, M. Fowler, S. Grot, Polymer 46 (25) (2005) 11707.